Bangalore

Article · September 2019

DOI: 10.1002/9781118568446.eurs0014

2 authors:

T V Ramachandra
Indian Institute of Science
1,183 PUBLICATIONS **14,925** CITATIONS

SEE PROFILE

Dr. Bharath H Aithal
Indian Institute of Technology Kharagpur
278 PUBLICATIONS **2,828** CITATIONS

SEE PROFILE

Some of the authors of this publication are also working on these related projects:

Project ISRO-IISC Space Technology Cell- Biofuel ISTC/BES/TVR/389 View project

Project Renewable Energy Potential Assessment View project

Bangalore

T. V. RAMACHANDRA
Indian Institute of Science, India

BHARATH H. AITHAL
Indian Institute of Technology Kharagpur, India

INTRODUCTION

Urbanization or urban growth is a dynamic process involving changes to vast expanses of land cover with the progressive concentration of human population. The process entails a switch from a spread-out pattern of human settlements to compact growth in urban centers. The process of urbanization gained impetus with the Industrial Revolution 200 years ago and accelerated in the 1990s with globalization and the consequent relaxation in the market economy. Rapidly urbanizing landscapes reach a huge population size leading to gradual collapse in urban services; the result is problems with housing, slums, lack of a treated water supply, inadequate infrastructure, higher pollution levels, poor quality of life, and so forth. Urbanization is a product of demographic explosion and poverty induced rural–urban migration. Globalization, liberalization, and privatization are the agents fueling urbanization in most parts of India. However, unplanned urbanization coupled with the lack of a holistic approach is leading to lack of infrastructure and basic amenities. Therefore, proper urban planning with operational, developmental, and restorative strategies is required to ensure the sustainable management of natural resources. The process of urbanization involves migration from rural to urban areas, increased urban population density, increased levels of consumption, corresponding lifestyle changes, and increased energy consumption; these shifts promote an increase in carbon emissions.

Urban growth is the spatial pattern of land development to accommodate anthropogenic demand that influences other land uses (e.g., open spaces, water bodies, etc.). The surface of the earth has been altered considerably by humans over the past 50 years through urbanization. On a global scale, 2.5 billion people were living in urban areas in 1950; the number is expected to be 6 billion by 2030 (Ramachandra, Aithal, and Durgappa 2012). Continuing urban growth raises concerns about the degradation of the environment and its ecological health. Understanding urban growth and change is critical to city planners and resource managers in these rapidly changing environments. Dynamic urban change processes, through which the productive agricultural lands, vegetation, and water bodies are irretrievably lost and transformed at an alarming rate is often referred to as rapid urbanization. Unplanned rapid urbanization changes the structure of the landscape, influencing its functioning quite apart from the lack of basic infrastructure, amenities, enhanced levels of pollution, and changes in local climate and ecology (Aithal and Ramachandra 2016a). This phenomenon is very rapid in India with its urban population growing at around 2.3 percent per annum, and certain cities like Bangalore have a higher population growth at 4.6 percent per annum (Ramachandra, Aithal, and Sowmyashree 2013). Cities in developing countries have grown more compact and more clustered, spreading beyond the boundaries of central cities (Ramachandra, Aithal, and Sowmyashree 2015). This dispersed growth close to the large urban forms having a mixed land use (Aithal and Ramachandra 2016a, 2016b) is known as "urban sprawl." This

leads to the inefficient use of land resources and energy and large-scale encroachment onto agricultural lands, traffic congestion, shortages in urban services and facilities, and major problems of urban poverty. Cities are expanding in all directions, which is resulting in large-scale urban sprawl and changes in urban land use (Ramachandra, Aithal, and Sowmyashree 2015). Large-scale land-use and land-cover changes combined with unplanned urbanization and sprawl has an impact on the environment and the sustainability of natural resources (Ramachandra, Aithal, and Barik 2014; Ramachandra, Aithal, and Sowmyashreeb 2014).

Understanding land-use and land-cover changes is essential to evolving appropriate strategies for sustainable management of natural resources and monitoring environmental changes such as greenhouse gas emissions and urban heat island effects (Ramachandra, Aithal, and Bharath 2013). Spatial data acquired through space-borne sensors since the early 1970s and advancements in geo-informatics have helped in understanding and visualizing landscape dynamics. The collection of remotely sensed data at regular intervals facilitates synoptic analyses of the earth: system function, patterning, and change at local, regional, and global scales over time. Further evaluating the impact of urban growth in this form on the environment and understanding the dynamics of complex urban systems involves modeling and simulation, which require innovative analytical methods and robust techniques. A number of analytical and static urban models have been developed that are based on diverse theories such as urban geometry, size relationship between cities, economic functions, and social patterns with respect to the city. However, these models explain urban expansion and evolving patterns instead of predicting future urban development. In urban modeling,

dynamic agent-based modeling as an urban simulation tool has rapidly gained popularity in recent years among urban planners and geographers. Considerable research efforts have developed different dynamic agent-based models (stochastic based on cellular automata, Markov model, etc.) for urban and environmental applications (Aithal, Vinay, and Ramachandra 2014). All these models have some common features, such as the use of transition probabilities in a class transition matrix (Aithal and Ramachandra 2016a). Cellular automata algorithms define the state of the cell based on the previous state of the cells within a neighborhood, using a set of transition rules. Coupled Markov chain (MC) and cellular automata (CA) eliminates the shortcomings of CA and MC respectively. MC quantifies future changes based on past changes, thereby serving as a constraint for CA, which addresses spatial allocation and the location of change. Although CA–Markov gives promising results, it fails to achieve accurate results since the driving forces are not accounted for in this model.

Fuzzy analytical hierarchical process (AHP)-based CA–Markov modeling uses analytical hierarchical process-based modeling to simulate the land-use dynamics based on the agents of change including drivers or constraints, socioeconomic and infrastructural activities, and human actions (Aithal, Vishwanatha, and Ramachandra 2015). Agent-based modeling (ABM) weights/ranks the growth factors and constraints as reflected by the real-world scenarios to develop site suitability maps in order to model the land use; it has emerged as a promising approach in understanding the complex urban processes. This provides ample opportunities and challenges which complement or extend to other approaches. The site suitability maps provide the transitional areas, describing where the particular land use has the probability to change or retain its state. The

site suitability maps are combined with the CA–Markov in order to simulate and predict the land-use dynamics.

Cities across the world with increased urbanization and urban populations also account for about two-thirds of the world's primary energy consumption and about three-quarters of the greenhouse gas (GHG) emissions. Concentration of greenhouse gases in the atmosphere has increased rapidly over the last century due to ever-increasing anthropogenic activity; this has resulted in significant increases in the temperature of the earth causing global warming. Major sources of GHG are transportation (burning of fossil fuel), forests (due to human-induced land-cover changes leading to deforestation), power generation (burning of fossil fuels), agriculture (livestock, farming, rice cultivation, and burning of crop residues), water bodies (wetlands), industry, and urban activities (building, construction, transport, solid and liquid waste). Aggregation of GHG (CO_2 and non-CO_2 gases), in terms of carbon dioxide equivalent (CO_2e), indicate the GHG footprint.

GHG footprint is a measure of the impact of human activities on the environment in terms of the amount of greenhouse gases produced. The study (Ramachandra, Aithal, and Shreejith 2015) calculated the amount of three important greenhouses gases, namely carbon dioxide (CO_2), methane (CH_4), and nitrous oxide (N_2O), thereby developing the GHG footprint of the major cities in India. Energy consumption and related GHG emissions in cities largely depend on how the cities grow and operate and on the sources of energy that are used to support these processes. Increased emissions of CO_2 and other greenhouse gases are the main contributors to global warming (Ramachandra, Aithal, and Shreejith 2015) with one-third of CO_2 emissions resulting from land-use changes. Rapid changes in land use leading to large-scale

degradation of natural resources (water bodies, tree cover) alter the carbon sink ability and affect the environment. Land-use change in the form of urbanization is a main factor that determines carbon dynamics and leads to global warming. Studies based on emissions and land use have established a correlation between global warming and enhanced emissions of greenhouse gases and urban heat island effect across the urbanizing regions in the world. Urban heat island (UHI) has been garnering substantial attention in recent decades. Extensive studies have been carried out to explore the impact of past urbanization on the UHI effect in cities with unique urban landscapes and histories – for example, Tokyo, Paris, New York City, Beijing, Houston, Singapore – using numerical models. This emphasizes the need for understanding spatial and temporal patterns of urbanization, land-use changes, greenhouse gas emissions, and urban heat island. This entry analyzes spatiotemporal patterns of urbanization in Bangalore, one of the most rapidly urbanizing cities with environmental sustainability issues.

STUDY AREA

Greater Bangalore, at 741 km^2, is the principal administrative, cultural, commercial, industrial, and educational capital of the state of Karnataka (Figure 1).

Bangalore is located at 12°59′ north latitude and 77°57′ east longitude, almost equidistant from the eastern and western coasts of the South Indian peninsula, and is situated at an altitude of 920 m above mean sea level. The mean annual total rainfall is about 900 mm. The summer temperature ranges from 18 to 38 °C, while the winter temperature ranges from 12 to 25 °C. Thus, Bangalore enjoys a salubrious climate around the year. With its numerous parks and abundant greenery, it was called the "garden
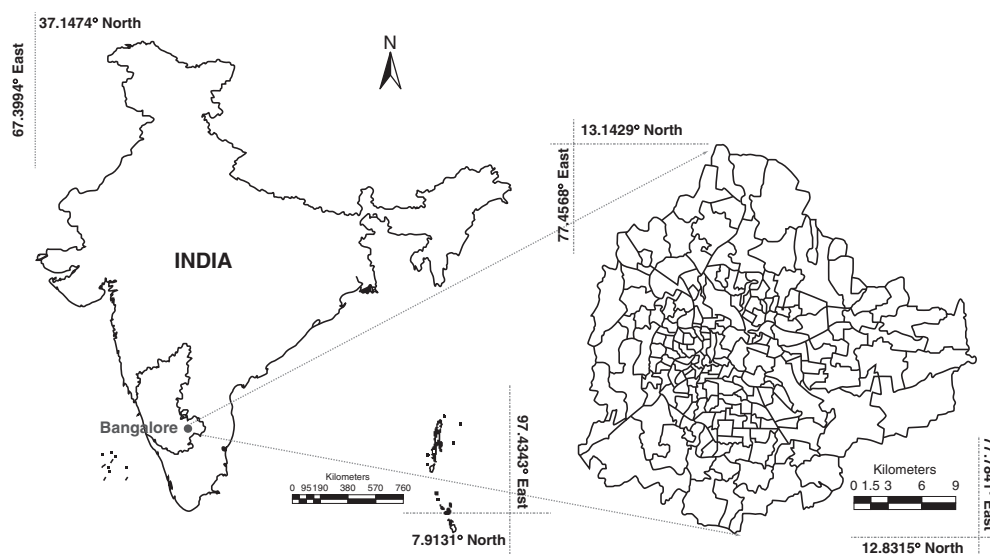
Figure 1 Study area: Bangalore (with 198 local administration wards)

city" of India. The Bangalore landscape is located over ridges forming three watersheds. The undulating terrain in the region has facilitated the creation of a large number of interconnected lakes.

Bangalore has grown by more than 10 times since 1951 (Figure 2). The present name of the city, Bangalore (Greater Bangalore), is an anglicized form of Bengalooru which according to popular belief is derived from *benda kaalu* or boiled beans and *ooru* meaning a town. In 1862 two independent municipal boards were established: Bangalore City Municipality, and Bangalore Civil and Military Station Municipality. In 1949, the two municipalities were merged and the Bangalore City Corporation was formed. Subsequently, there have been reorganizations with respect to the zones and wards within the corporation, rising from 50 divisions in 1949 to 95 wards in the 1980s, 100 wards in 1995, and now about 150 wards. In 2006 the Bangalore City Corporation was reorganized as Greater Bangalore City Corporation with 198 wards.

The urban agglomeration had an overall population in 2011 of 8.4 million (Figure 2), including a workforce of 6.2 million, and a literacy rate of 87.6 percent according to the latest census. The information and technology (IT) sector is a major employer with 45 percent of the workforce and the highest per capita income in the state at 202,176 rupees (State and District Domestic Product of Karnataka 2016). This has significantly increased people's purchasing power and has encouraged the growth of real estate with consequent land market dynamics, as well as creating a lot of secondary employment in the service industries.

Bangalore is home to numerous high-tech knowledge hubs. This is evident from the establishment of premier centers like the Indian Institute of Science (IISc), Indian Space Research Organisation (ISRO), National Aerospace Laboratories (NAL), Defence Research and Development Organisation (DRDO), and Indian Institute of Management (IIM). The city also houses a huge number of professional engineering and medical colleges at undergraduate and graduate
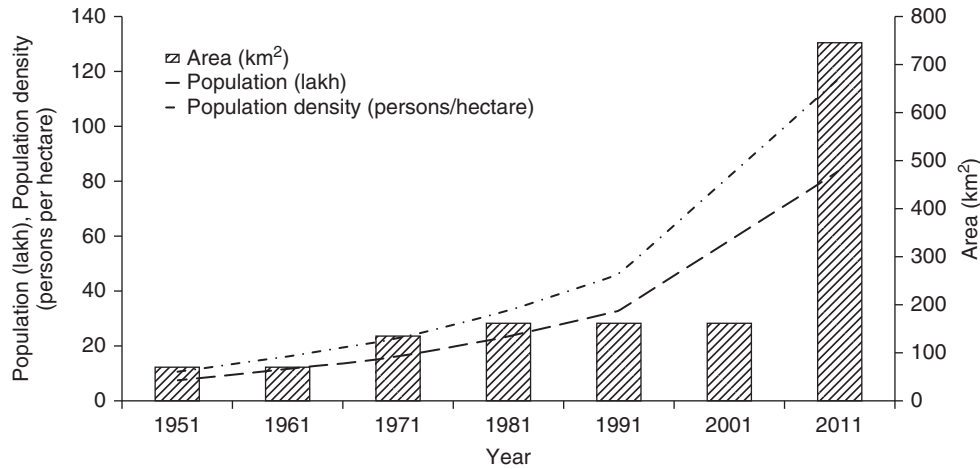
Figure 2   Spatial and population dynamics in Bangalore, 1951 to 2011. Note: Population is in lakhs; one lakh = 0.1 million

levels. An important feature of the economic activities of Bangalore is the huge concentration of small and medium enterprises (SMEs) in diversified sectors across the city. Thus the city has a thriving economy with a gross domestic product of US$83 billion. The city is also branded the country's "Silicon Valley" because of its remarkable contributions in technological innovation and its high HDI (human development index) of 0.73 (Karnataka Human Development Report 2005).

Bangalore's urban vegetation includes trees such as *Alstonia scholaris*, *Artocarpus heterophyllus* (jackfruit), *Azadirachta indica* (neem), *Bombax cieba* (red silk cotton), *Butea monosperma*, *Ficus bengalensis* (alada mara), *F. religiosa* (ashwatha), *Gmelina arborea*, *Kigelia pinnata* (sausage tree), *Lagerstroemia speciosa* (pride of India), *Mangifera indica* (mango), *Madhuca longifolia* (mehwa or ippe), *Melia composite* (Malabar neem), *Michelia champaca*, *Neolamarkia kadamba* (kadamba), *Pongamia pinnata* (honge), *Pterocarpus marsupium* (honne), *Syzigium cumini* (jaamun), *Saraca indica* (seeta asok), *Swetenia* sp. (mahogani), *Terminalia arjuna* (arjuna), *T. bellerica* (tare), *Tabebuia spectabilis*, and

many more. Some of the gracious exotic trees found as avenue trees are *Delonix regia* (gulmhur), *Enterolobium saman* (rain tree), *Parkia biglandulosa* (badminton ball tree), *Peltophorum pterocarpum* (copper pod), *Spathodea companulata* (African tulip tree), *Tabebuia spectabilis*, and *Polythia longifolia*.

DATA

Urban dynamics were assessed using temporal remote sensing data for the period 1973 to 2010. The time series spatial data acquired from Landsat Series Multispectral Sensor (57.5 m) and Thematic Mapper (28.5 m), OLI (28.5 m) sensors for the period 1973–2016 were downloaded from the public domain. The Survey of India (SOI) topographic maps of 1:50,000 and 1:250,000 scales were used to generate base layers of city boundary and other details. City maps with ward boundaries were digitized from the BBMP (Bruhat Bangalore Mahanagara Palike) map. Ground control points to register and geo-correct remote sensing data were collected using handheld pre-calibrated

GPS (global positioning system), the SOI topographic maps, and online spatial portals.

Wetland delineation was performed using field data collected with a handheld GPS. Remote sensing data used for the study are: Landsat MSS data of 1973, Landsat TM of 1992, Landsat ETM+ of 2000 MODIS 7 bands product of 2002 and 2007 downloaded from the online portal, IRS LISS-3 data of 2006 procured from NRSA, Hyderabad. India Google Earth data served in the pre- and post-classification process and validation of the results.

Vegetation cover analysis was done using Indian remote sensing (IRS) satellite Resourcesat 1 (multispectral with spatial resolution of 5.8 m) and Cartosat 1 (panchromatic with spatial resolution 2.7 m). These data were fused using hyperspectral color space resolution merge for better spatial and spectral resolution based on the universal image quality index (UIQI).

METHOD

This includes understanding spatial patterns of urban growth, geovisualization of urban dynamics, vegetation cover analysis, delineation of water bodies, sector-wise analysis of greenhouse gas footprint, changes in land surface temperature, and urban heat island.

Spatial pattern of urban growth in Bangalore

The remote sensing data obtained were geo-referenced, rectified, and cropped pertaining to the city boundary (study area). Geo-registration of remote sensing data (Landsat data) was done using ground control points collected from the field using precalibrated GPS and also from known points (such as road intersections, etc.) collected from geo-referenced topographic maps published by the Survey of India. The

Landsat satellite 1973 images with a spatial resolution of 57.5 m × 57.5 m (nominal resolution) were resampled to 28.5 m comparable to the 1989–2016 data which are 28.5 m × 28.5 m (nominal resolution). Landsat ETM+ bands of 2010 were corrected for the SLC-off by using image enhancement techniques, followed by nearest-neighbor interpolation.

Land-use classification using remote sensing data involved (a) generation of false color composite (FCC), which helped in identifying and locating heterogeneous patches of landscapes; (b) selection of training data from the FCC (the training sites should cover at least 15 percent of the total area and be distributed over the study area); (c) loading of these training data sites as polygon features to a GPS for collection of attribute information for the training data sites from the field; (d) supplementation of the information using Google Earth. Seventy percent of the training data were used for classification and the rest for validation of the classified outputs and accuracy assessment. The classification of the data was completed using GRASS (Geographic Resource Analysis Support System) open source GIS software by considering four prime land-use classes.

Land-use analysis was carried out using supervised pattern classifier Gaussian maximum likelihood algorithm as in Figure 3. This has been proved a superior classifier as it uses various classification decisions using probability and cost functions (Ramachandra, Aithal, and Durgappa 2012). Mean and covariance matrix are computed using estimate of maximum likelihood estimator. Accuracy assessment to evaluate the performance of classifiers was done with the help of field data by testing the statistical significance of a difference, computation of kappa coefficients, and proportion of correctly allocated cases. Recent remote sensing data were classified using the collected training samples. Statistical assessment

of classifier performance, based on the performance of spectral classification considering reference pixels, was done which included computation of kappa (κ) statistics and overall (producer's and user's) accuracies. For earlier time data, training polygon along with attribute details were compiled from the historical published topographic maps, vegetation maps, revenue maps, and so on.

Land-use categories include (a) area under vegetation (parks, botanical gardens, grasslands such as golf courses), (b) built-up (buildings, roads, or any paved surface, (c) water bodies (lakes/tanks, sewage treatment tanks), and (d) others (open areas such as playgrounds, quarry regions, etc.) (see Table 1).

Modeling and visualization of urban growth

Agent-based modeling was used in the form of fuzzy (to understand the behavior of the agent) as an input, analytical hieratical process (AHP) was used to create the agents' influence in the region, and CA–Markov to model the land-use transition. Influencing agents were prioritized which include slope, proximity to roads, industry, educational institutions, and bus, railway, and metro stations. Factors such as hospitals and sociocultural buildings have a minimal role in urbanization. All these factors were generalized using a fuzzy analytical process and prioritized using AHP in order to weight the

factors based on land use type. The weightages from the AHP and the constraints as Boolean were used to generate transition suitability maps for different land use using multi-criteria evaluation (MCE) technique (Figure 3). The transition suitability (of MCE) along with transition probabilities (from Markov) (were used to calibrate the parameters and simulate the sprawl for the most recent data based in cellular automata using CA–Markov transitions. Validation of the simulated output was carried out with respect to the classified data for recent data. Calibrated parameters were further used to derive the land use for the year 2020.

CA–Markov: Markov chains were used to establish the transition probabilities to estimate the area under change based on the transition rules incorporated with the land use. Cellular automata were used to obtain a spatial location and distribution of probable land-use changes based on associated and surrounding pixels. The probability/site suitability map from cellular automata and the transition probabilities were used in convergence in order to simulate the future land-use scenarios.

Fuzzy AHP/CA–Markov: Modeling, simulation, and prediction of the land use dynamics were carried out using the combination of fuzzy logic, analytical hierarchical process (AHP), Markov chains and cellular automata. Factors that have an impact on urbanization include roads, industries, educational institutions, bus stands, railway

Table 1 Land-use categories

Land use	Categories included in land use
Urban	Residential areas, industrial areas, paved surfaces, mixed pixels with built-up area
Water	Tanks, lakes, reservoirs, drainages
Vegetation	Forest, plantations
Other	Rocks, quarry pits, open ground at building sites, unpaved roads, croplands, nurseries, bare land
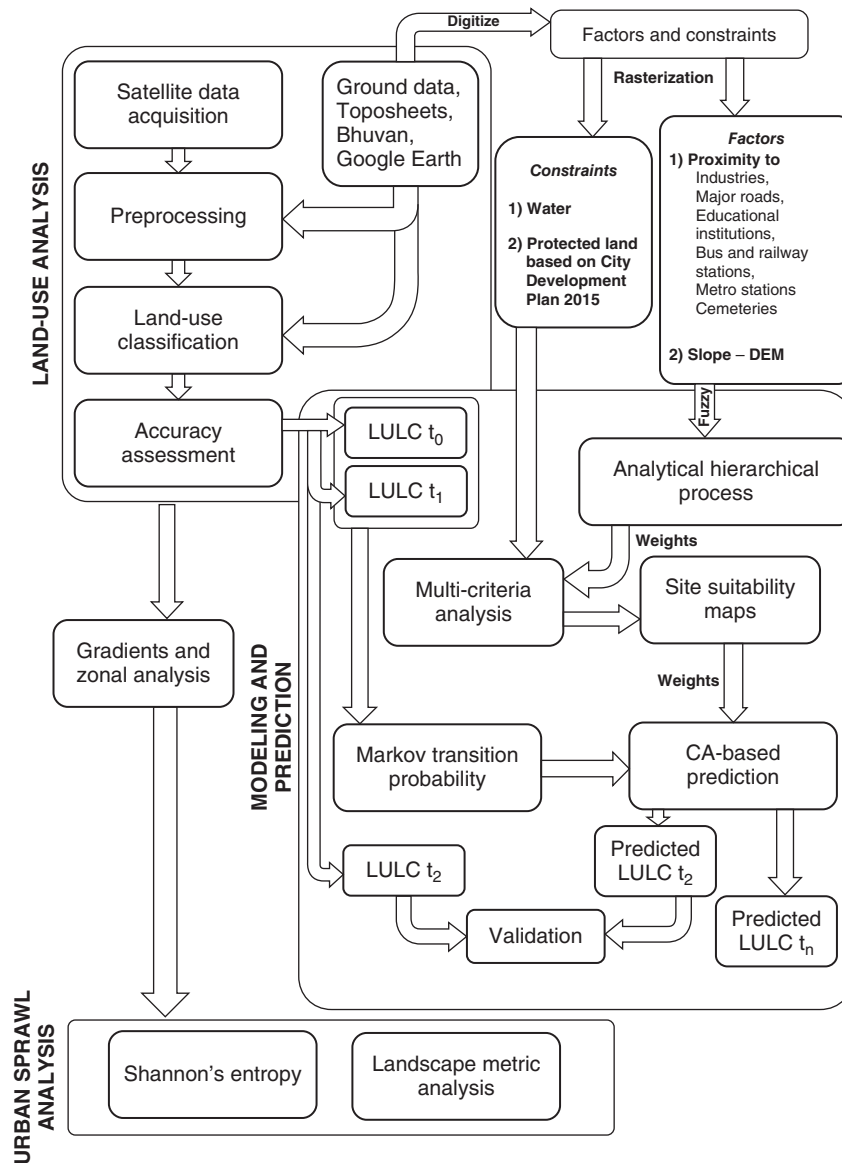
Figure 3 Flowchart illustrating the method of land-use analysis and visualization

stations, metro, population, city development plan (CDP), and water bodies were taken into consideration. Fuzzy logic was used to normalize factors such as slope, proximity maps (proximity to road, proximity to industries, proximity to educational institutions, proximity to bus stands, etc.) between 0 to 255, and

Boolean algebra was used on constraining factors of development such as water bodies and CDP where the restricted locations for any new change would be zero vice versa. Factors of growth were prioritized/ranked and their effectiveness in change in land use was estimated/mapped using the AHP.

Prioritized weighted factors of growth along with the constraints were combined together through the multi-criteria evaluation process to derive site suitability maps. Site suitability maps provide an insight into how the land use can be managed. The site suitability maps along with the Markov transition probabilities are used in order to simulate the land use for the year 2016 and predict across further years. Both the above section on land use and visualization can be summed up as in Figure 3.

Vegetation cover analysis

Vegetation cover analysis was done using Indian remote sensing (IRS) satellite Resourcesat 1 (multispectral with spatial resolution of 5.8 m) and Cartosat 1 (panchromatic with spatial resolution 2.7 m). This involved (a) data fusion, (b) classification, and (c) analysis of tree distribution:

(a) *Data fusion*: Fusion of data from multiple sensors aids in delineating objects with comprehensive information due to the integration of spatial information present in the high resolution (HR) panchromatic (PAN) image and spectral information present in the low resolution (LR) multispectral (MS) images. Image fusion techniques integrate both PAN and MS and can be performed at pixel levels. Data fusion (Resource sat and Cartosat data) was performed using algorithms: Hyperspectral Color Space resolution (HCS) merge, High Pass Filter (HPF) fusion, Modified Intensity Hue Saturation (MIHS) fusion, Wavelet Fusion.

The output of different fusion methods was analyzed for better accuracy and similarity in original data and fused data using the UIQI index. Universal image quality index (UIQI) is used to measure the similarity between two images. UIQI measures image distortion as a combination of three major factors: loss of correlation between data sets, radiometric imbalance, and contrast distortion. UIQI index was calculated using equation 1:

$$\text{UIQI} = Q = \frac{\sigma_{AB}}{\sigma_A \sigma_B} * \frac{2\mu_A \mu_B}{\mu^2_A + \mu^2_B}$$
$$* \frac{2\sigma_A \sigma_B}{\sigma^2_A + \sigma^2_B}$$

(equation 1)

HCS is more sensitive to image co-registration accuracy. Inaccurate co-registration may result in blurring edges in the fused images. The MIHS transform fusion techniques are not sensitive to the co-registration accuracy as the textural features are replaced by the intensity replacement image. The visual evaluation and statistical analysis confirm that HCS is a superior fusion technique for improving spatial detail of MS images with the preservation of spectral properties.

(b) *Classification*: The land-use analysis was carried out to classify the data into two classes, namely vegetation (trees) and nonvegetation, using the fused high spectral and spatial remote sensing data through the Gaussian Maximum Likelihood Classifier (MLC) algorithm with the help of training data acquired from the field and supplementary data from Google Earth. The MLC classifier uses the probabilities to classify each pixel into a particular land-use class. The Gaussian MLC classification technique (Ramachandra et al., 2011; Ramachandra, Aithal, and Sowmyashree 2013) has been used widely for analysis of land use as this technique has proved to be superior to other classification techniques.

(c)   *Analysis of tree distribution*: The analysis of tree distribution was carried out based on frequency distribution of the tree canopy area. The method involved in assessing the distribution includes: data collection, frequency distribution, tree distribution in each ward:

- *Data collection:* Five wards including the Indian Institute of Science campus (178 hectares, 22,000 trees) were sampled. The spatial extent of trees (with canopy size) covered under different species in selected wards was delineated using pre-calibrated GPS and Google Earth. This aided in delineating canopies of trees based on k-means algorithm in all wards (198 wards). The canopy area was used to determine the frequency distribution of trees with respect to the crown area in each ward.
- *Frequency distribution:* Based on the field data, wards were categorized into > 500 trees and < 500 trees. The frequency distribution of number of trees versus average area of a tree was analyzed to determine the statistical distribution of tree species in the respective ward.
- *Tree distribution in each ward:* The frequency distribution under each category was used to quantify the actual number of trees in each ward. The population for the year 2013 was estimated for each ward (equation 2) based on the decadal growth to determine the tree distribution per person in each ward:

$$P_{2013}(i) = P_{2011}(i) * (1 + n * r(i))$$
$$\text{(equation 2)}$$

where $P_{2013}(i)$ = population of ward i for the year 2013; $P_{2011}(i)$ =

population of ward i for the year 2011; n = number of decades = 0.2; r(i) = incremental rate of ward i.

The ratio of number of trees in each ward to population in each ward was determined to quantify tree distribution per person in each ward using equations 3 and 4:

$$\text{TpP}(i) = \frac{\text{Tree}(i)}{P_{2013}(i)} \quad \text{(equation 3)}$$

$$\text{TpP}(B) = \frac{\sum_{i=1}^{198} \text{Tree}(i)}{\sum_{i=1}^{198} P_{2013}(i)}$$
$$\text{(equation 4)}$$

where TpP(i) = tree per person in ward i; Tree(i) = number of trees in ward i; TpP(B) = trees per person in Bangalore.

- *Validation:* The validation was carried out with the field data using GPS. Accuracy assessment was carried out using equation 5:

$$\text{Accuracy} =$$
$$100 - (\text{abs}((\text{Class}_{\text{Tree}} - \text{GPS}_{\text{Tree}})/$$
$$\text{GPS}_{\text{Tree}}) * 100) \quad \text{(equation 5)}$$

where $\text{Class}_{\text{Tree}}$ = tree count based on classified data; GPS_{Tree} = tree count based on field census using GPS.

Delineation of wetlands of Bangalore

K-means algorithm was used to partition the data samples in the feature space into disjoint subsets or clusters. Accuracy assessment of automatically extracted wetlands was done with field knowledge, visual interpretation, and Google Earth.

Greenhouse gas (GHG) footprint assessment

The method involved (a) sector-wise quantification of GHG emissions, (b) computation of carbon dioxide equivalent (CO_2e) of the non-CO_2 gases using their respective global warming potential (GWP), and (c) aggregation of these CO_2e to represent the GHG footprint. The major three greenhouse gases quantified were carbon dioxide (CO_2), methane (CH_4), and nitrous oxide (N_2O). The non-CO_2 gases are converted to units of carbon dioxide equivalent (CO_2e) using their respective global warming potential (GWP), representing the GHG footprint. The total units of CO_2e then represent a sum total of the global warming potential of all three major greenhouse gases, which represents the GHG footprint. The major categories considered for GHG emission inventory are energy (electricity consumption, fugitive emissions); the domestic or household sector; transportation; the industrial sector; agriculture-related activities; livestock management; the waste sector.

National greenhouse gas inventories compiled from various sources were used for calculation of GHG emissions. Country-specific emission factors were compiled from the published literature. In the absence of country-specific emission factors, default emission factors of IPCC were used. Emission of each GHG was estimated by multiplying fuel consumption by the corresponding emission factor. Total emissions of a gas from all its source categories, emissions are summed as given in equation 6:

$$\text{Emissions}_{Gas} = \sum_{Category} A \times EF$$
(equation 6)

where Emissions_{Gas} = emissions of given gas from all its source categories; A = amount of individual source category utilized which generates emissions of the gas under consideration; EF = emission factor of a given gas type by type of source category.

Land surface temperature (LST) and urban heat island

Digital number (DN) of Landsat ETM+ was converted into spectral radiance L_{ETM} using equation 7, and then converted to at-satellite brightness temperature (i.e., black body temperature, $T_{ETMSurface}$), under the assumption of uniform emissivity ($\varepsilon \approx 1$) using equation 8:

$$L_{ETM} = 0.0370588 \times DN + 3.2$$
(equation 7)

$$T_{ETMSurface} = K_2 / \ln\left(K_1 / L_{ETM} + 1\right)$$
(equation 8)

where $T_{ETMSurface}$ is the effective at-satellite temperature in Kelvin, L_{ETM} is spectral radiance in watts/(meters squared × ster × μm); and K_1 and K_2 are pre-launch calibration constants. For Landsat-7 ETM+, K_2 = 1282.71 K and K_1 = 666.09 $mWcm^{-2}sr^{-1}\mu m^{-1}$ were used (https://landsat.gsfc.nasa.gov/landsat-7-science-data-users-handbook/). The emissivity corrected land surface temperatures Ts were finally computed by equation 9:

$$T_s = \frac{T_B}{1 + \left(\lambda \times T_B / \rho\right) \ln \varepsilon}$$
(equation 9)

where λ is the wavelength of emitted radiance for which the peak response and the average of the limiting wavelengths ($\lambda = 11.5\,\mu m$) were used; $\rho = h \times c/\sigma$ (1.438×10^{-2} mK); σ = Stefan–Boltzmann constant (5.67×10^{-8} $Wm^{-2}K^{-4} = 1.38 \times 10^{-23}$ J/K); h = Planck's constant (6.626×10^{-34} Jsec); c = velocity of light (2.998×10^8 m/sec); and ε is spectral emissivity.
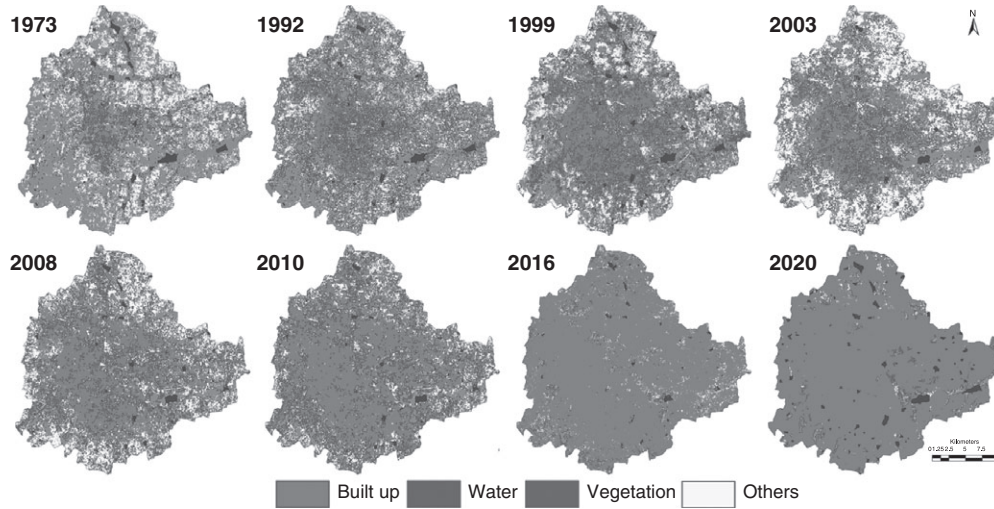
Figure 4   Urban dynamics in Bangalore and visualization of growth by 2020

RESULTS AND DISCUSSION

Land-use analysis

Figure 4 depicts the unrealistic urban growth during the last two decades. Overall accuracy of the classification was 72 percent (1973), 77 percent (1992), 76 percent (1999), 80 percent (2002), 75 percent (2006), and 78 percent (2010) respectively. Urbanization during the period 1973 to 2016 (1005 percent concretization or paved surface increase) has telling influences on the natural resources such as decline in green spaces (88 percent decline in vegetation) and wetlands (79 percent decline). Analyses of the temporal data reveal an increase in urban built-up area of 342.83 percent (1973 to 1992), 129.56 percent (1992 to 1999), 106.7 percent (1999 to 2002), 136.92 percent (2002 to 2008), 105.19

percent (2008 to 2010), and 147.13 percent (2010 to 2016) and land use is as shown in Table 2.

Geo-visualization of urban growth

The transition suitability (of MCE) along with transition probabilities (from Markov) were used to calibrate the parameters and simulate the sprawl for the year 2016 based on cellular automata using CA–Markov transitions. Validation of the simulated output was carried out with respect to the classified data for 2016. The simulated model for 2016 closely agrees with that of the classified land use with kappa of 0.86. The calibrated parameters were further used to derive the land use for 2020. This prediction has been done assuming water bodies to remain constant over all time frames, due

Table 2   Land-use statistics of urban pattern in Bangalore

Class	1973	1992	1999	2002	2008	2010	2016	2020
Built-up	7.97%	27.30%	35.37%	37.74%	49.54%	54.42%	76.91%	93.26%
Vegetation	68.27%	46.22%	45.77%	38.72%	28.19%	23.41%	7.53%	2.96%
Water	3.40%	2.62%	2.26%	1.85%	0.86%	0.90%	0.98%	2.09%
Others	20.35%	23.86%	16.61%	21.70%	21.41%	21.27%	14.59%	1.69%

to recent stringent norms. The simulation shows a predominant growth along the east and south directions showing the effect of upcoming industrial hubs in these directions. The process of urbanization in the simulated results is evident along the arterial roads and at the core of the city; the built-up density increases in lateral directions to a very large extent almost to the verge of being saturated, followed by gradual sprawl along the boundary of the city. Geo-visualization of likely land uses in 2020 through multi-criteria decision-making techniques (fuzzy AHP) reveals a calamitous picture of 93 percent of the Bangalore landscape filled with paved surfaces (urban cover) and drastic reduction in open spaces and green cover (Table 2 and Figure 4).

Wetlands of Bangalore

The latest field survey (2015–2016) of lakes reveals that 98 percent of lakes have been encroached on by illegal buildings (high rise apartments, commercial buildings, slums, etc.); 90 percent of lakes are sewage fed; 38 percent are surrounded by slums; and 82 percent showed loss of catchment area. Also, lake catchments were used as dumping grounds for municipal solid waste or building debris. The surroundings of these lakes have illegally constructed buildings and slum-dwellers occupy most of the adjoining areas. At many sites, water is used for washing and household activities, and fishing was even observed at one of these sites. Multistoried buildings have come up on some lake beds, affecting the natural catchment flow and thus leading to a deteriorating quality of water bodies. Unauthorized construction in valley zones, lake beds, and storm water drains (rajakaluves) highlight the apathy of decision-makers while revealing weak and fragmented governance. This is correlated with the increase in concreted areas which severely affect open spaces

Table 3   Status of water body of Bangalore

	Bangalore city (BMP, before 2004)	Greater Bangalore
1973	58	207
2010	10	93

and, in particular, water bodies. Figure 5 and Table 3 show that Greater Bangalore had 207 water bodies in 1973, which had declined to 93 in 2010. The Bangalore landscape forms an important catchment for the lake system and the present status of drains is reflected in Figure 6. These interconnected lake systems with their drainage networks help in transporting storm water beyond the city limits. Bangalore, being a part of peninsular India, had the tradition of harvesting water through surface water bodies to meet domestic water requirements in a decentralized way. These lake systems also helped in recharging groundwater resources. The groundwater table has declined to 300 m from 28 m (with the removal of water bodies) and 400 to 500 m in intensely urbanized areas such as Whitefield over a period of 20 years with the decline in wetlands and green spaces. Bangalore depends on the groundwater resources to an extent of 40 percent. The disappearance of local water sources and consequent decline in the groundwater table have led to a severe water scarcity in the region.

Vegetation status

The vegetation cover in the city depicted in Figure 7 was derived from the fused remote sensing data (MSS IRS data of 5.8 m and Cartosat data of 2.7 m) using the MLC classifier. This highlights that the vegetation cover is about 100.02 hectares (14.08 percent). Accuracy assessment of classified data shows an overall accuracy was 91.5 percent, the kappa of 0.86 indicating higher agreement of classified data with field reference data:
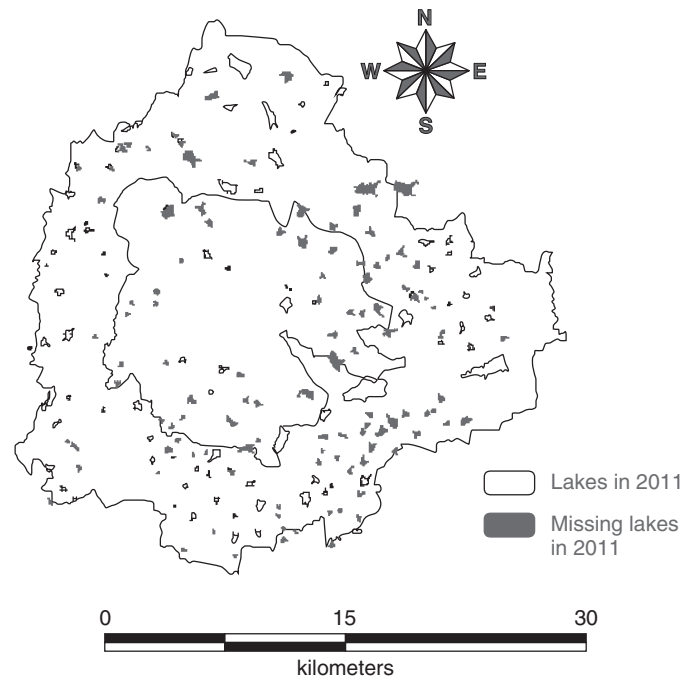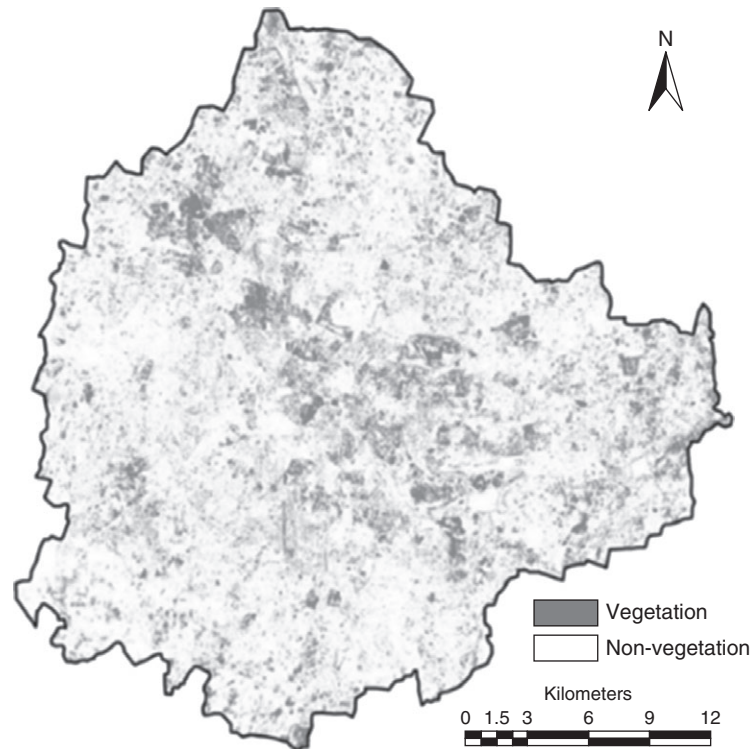
Figure 5 Missing urban sinks

**Figure 6** Interlinked lake systems of Bangalore with catchment boundary

**Figure 7**   Spatial distribution of vegetation in Bangalore

- *Spatial patterns of vegetation cover*: Bangalore was divided into 1 km radius circles (with respect to the central business district) to assess the vegetation gradient. Figure 8 depicts vegetation density in each concentric region in 1973 and 2013. Bangalore has an average vegetation density of 0.14 (i.e., area of Bruhat Bangalore: 741 km², area under vegetation: 100.20 km² and vegetation density: 0.14). Vegetation extent in each ward was computed by overlaying the ward boundary, as shown in Figure 9. Wards such as Hudi, Aramane nagara, and Vasantha pura have higher vegetation density of more than 0.4, while Chickpete, Laggere, Hegganahalli, Hongasandra, and Padarayanapura have lower density with less than 0.015.

Greenhouse gas emissions

The GHG footprint (aggregation of carbon dioxide equivalent emissions of GHGs) was 19796.5 Gg (19.796 million tonnes) and the major contributing sectors are the transportation (43.48 percent), domestic (21.6 percent), and industrial sectors (12.31 percent). Figure 10 shows the contributions of various sectors to the city's GHG footprint. Emissions from transport are due to the large-scale use of private vehicles, and mobility related to jobs accounts for 60 percent of total emissions due to the lack of an appropriate public transport system and haphazard growth with unplanned urbanization. There is a lack of integrated land use and mobility planning, and therefore the majority of people commute long distances,
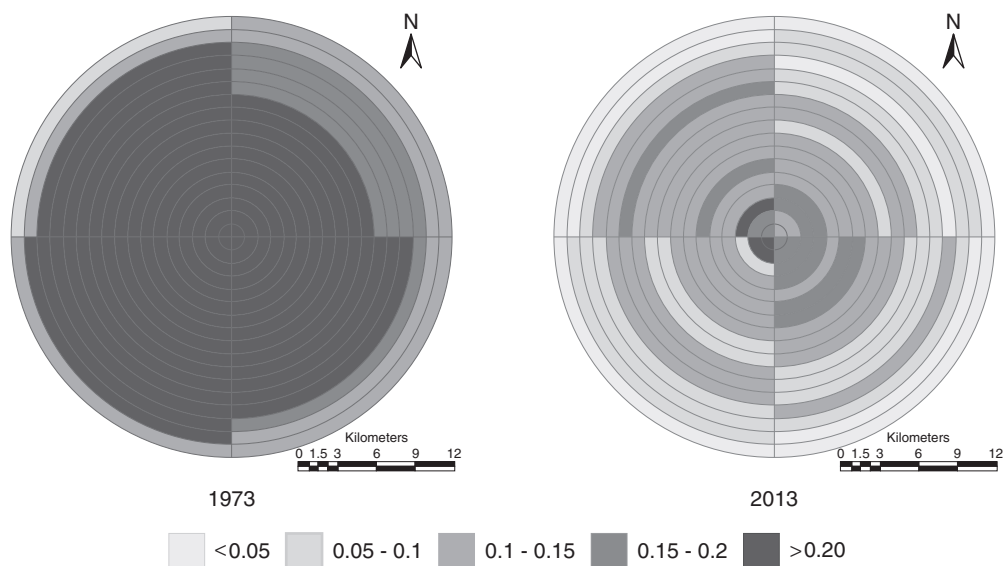
Figure 8 Gradient-wise vegetation density
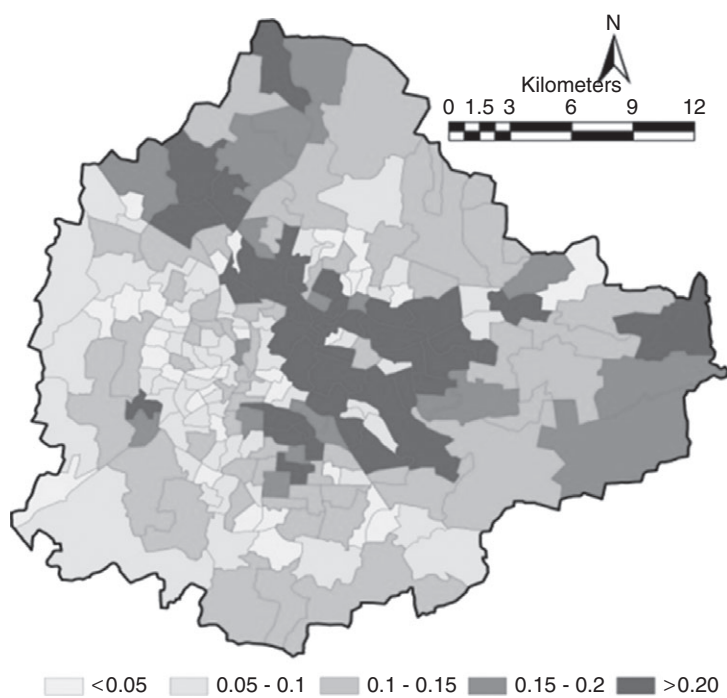
Figure 9 Ward-wise vegetation density (2013)
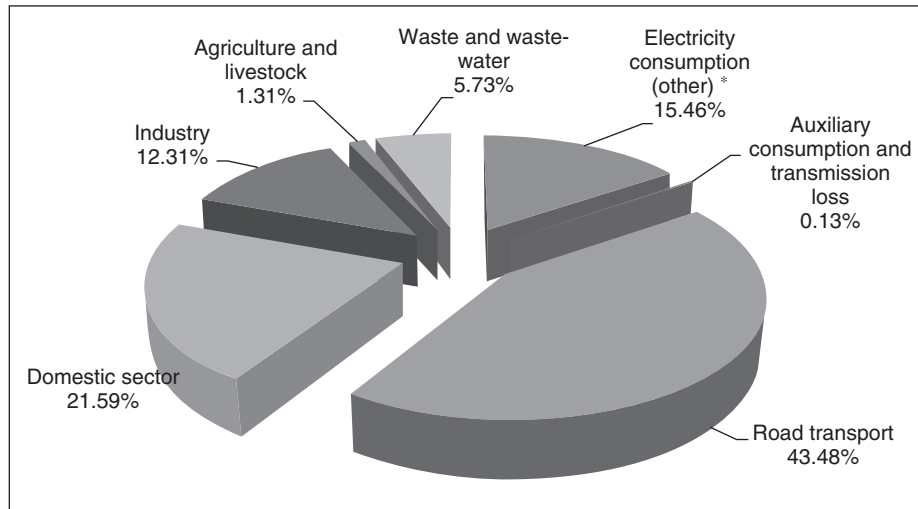
Figure 10   GHG emissions sector-wise

thus contributing to emissions. Higher fuel consumption, enhanced pollution levels due to the increase of private vehicles, and traffic bottlenecks have contributed significantly to carbon emission. The consumption of electricity has drastically increased in certain corporation wards with the adoption of inappropriate building architecture for the tropical climate region. This is evident from higher per capita electricity consumption in the zones dominated by high rise buildings with glass facades, which require 14,000–17,000 units (kWh) per year compared to the zones with eco-friendly buildings (1300–1500 units/person/year). In addition, mismanagement of solid and liquid wastes has aggravated the situation. Dumping of untreated solid and liquid waste into the water bodies has increased the anaerobic condition, leading to emission of greenhouse gases (methane, CO_2, etc.).

Land surface temperature and urban heat island

Temporal analysis of LST shows a gradual increase from 19.03 ± 1.47 °C (in 1991), 26.57 ± 1.25 (2000), 31.24 ± 2.21 (2007), to 37.14 ± 2.68 °C (2016) with the increase in paved surfaces in the city. Relatively lower temperatures in the regions with vegetation cover (25.79 ± 0.44), 24.20 ± 0.27 (water bodies) highlights the role of natural resources in moderating the local climate. Urban heat islands are formed with the increase of surface and atmospheric temperatures due to anthropogenic heat discharge due to energy consumption, increased land surface coverage by artificial materials having high heat capacities and conductivities, radiation by buildings due to inappropriate architecture, and the drastic decline in vegetation and water pervious surfaces (which aid in reducing the surface temperature through evapotranspiration, etc.). The implication for local climate is evident, with an increase of ~2.5 to 3 °C temperature during the last two decades) with the decline of natural resources (decline in vegetation cover and disappearance of water bodies) that aided in moderating the local climate.

CONCLUSION

Cities' origins can be traced back to the river valley civilizations of Mesopotamia, Egypt, the Indus Valley, and China. Initially these settlements were largely dependent upon agriculture; however, with the growth in population the city size increased and economic activity transformed to trading. The process of urbanization gained impetus with the Industrial Revolution 200 years ago and accelerated in the 1990s with globalization and consequent relaxations in the market economy. Migration to urban areas pushed the growth of towns and cities with the hope of better living standards, considering relatively better infrastructural facilities (education, recreation, health centers, banking, transport, and communication) and higher per capita income. However, unplanned urbanization leads to large-scale land-use changes affecting the sustenance of local natural resources. Hence, understanding spatial patterns of changes in the land and advance visualization of growth is imperative for sustainable management of natural resources and mitigation of changes in climate. This would help the city planners when planning how to mitigate the problems associated with the increased urban area and population, and ultimately to build sustainable cities.

Bangalore has experienced unprecedented rapid urbanization and sprawl, which has led to large-scale land-cover changes and associated serious environmental degradation, posing serious challenges to the decision-makers in the city planning and management process and involving many serious challenges such as climate change, enhanced greenhouse gases (GHG) emissions, lack of appropriate infrastructure, traffic congestion, and lack of basic amenities (electricity, water, and sanitation) in many localities. Temporal analyses of urbanization using temporal remote sensing data

from 1973 to 2016 reveals 1005 percent concretization (or paved surface increase) with a decline in green spaces (88 percent decline in vegetation), wetlands (79 percent decline), higher air pollutants, and a sharp decline in the groundwater table. Quantification of the number of trees in the region using remote sensing data with field census reveals that there are only 1.48 million trees to support Bangalore's population of 9.5 million, indicating one tree for every seven persons in the city. This is insufficient even to sequester respiratory carbon (540–900 g per person per day). Geo-visualization of likely land uses in 2020 through multi-criteria decision-making techniques (fuzzy AHP) reveals a calamitous picture of 93 percent of the Bangalore landscape filled with paved surfaces (urban cover) and drastic reduction in open spaces and green cover. This would make the region GHG rich, water scarce, nonresilient, and unliveable, depriving city-dwellers of clean air, water, and environment. Major implications of unplanned urbanization are (a) loss of natural resources, (b) groundwater decline, (c) altered regional hydrology and recurring episodes of floods, (d) enhanced GHG footprint and significant contributions to global warming, (e) reduced carbon sequestration (with the removal of tree cover and water bodies), (f) alterations in micro climate, (g) heat island formation, (h) escalated energy consumption, (i) mismanagement of solid and liquid waste generated in the region, (j) health impacts (increased instances of kidney failure, respiratory ailments, cancer, etc.), (k) aggressive behavior of humans (leading to frequent unrest with intra-family and societal conflicts), and (l) domination of anti-social gangs with the fragmented governance of local administration.

Conversion of wetlands to residential and commercial areas has compounded the problem by removing the interconnectivities in an

undulating terrain. Encroachment of natural drains, alteration of topography involving the construction of high rise buildings, removal of vegetative cover, and reclamation of wetlands are the prime reasons for frequent flooding even during normal rainfall post-2000. Field investigations (during 2015–2016) of 105 lakes revealed that 98 percent of lakes have been encroached upon for illegal buildings, 90 percent of lakes are sewage fed, 38 percent surrounded by slums and 82 percent showed loss of catchment area. Also, lake catchments are being used as dumping yards for either municipal solid waste or building debris. Indiscriminate disposal of solid and liquid waste (rich in organic nutrient) has enriched nitrate levels in the surrounding groundwater resources, threatening the residents' health (such as kidney failure, cancer, etc.). Washing, household activities, vegetable cultivation, and even fishing were observed in some contaminated lakes. Multi-storied buildings have come up on some lake beds, interfering in the natural catchment flow and leading to a deteriorating quality of water bodies. Unauthorized construction in valley zones, lakebeds, and storm water drains highlights the apathy of decision-makers while mirroring weak and fragmented governance. This correlates with the increase in unauthorized constructions violating town-planning norms (city development plan) which has affected severely open spaces and in particular water bodies. Large-scale fish mortality in recent months further highlights the level of contamination and irresponsible management of water bodies. Sustained inflow of untreated sewage has increased the organic content beyond the threshold of remediation capability of respective water bodies. Increasing temperature (of 34 to 35 °C) with the onset of summer enhanced the biological activities (evident from higher biochemical

oxygen demand and ammonia) that lowered dissolved oxygen levels leading to fish death due to asphyxiation. Thus, unplanned urbanization not only contributes to global climate change by emitting the majority of anthropogenic greenhouse gases but also is particularly vulnerable to the effects of climate change and extreme weather. This emphasizes the need to improve urban sustainability through innovation while addressing technical, ecological, economic, behavioral, and political challenges to create cities that are low carbon, resilient, and liveable.

The "smart cities" mission launched by the government in India recently (June 2015) envisages developing physical, institutional, and social infrastructure in select cities with central assistance targeted at improving the quality of life as well as economic visibility of the respective urban centers. Four strategic key components are:

1. greenfield development through smart townships by adopting holistic land management;
2. pan-city development through adoption of smart applications like transport, reuse and recycling of wastewater, smart metering, recovering energy from solid waste, etc.;
3. retrofitting, to make existing areas more efficient and liveable by reducing the greenhouse gas footprint, improving power and treated water supply, improving communication and infrastructure connectivity, and security;
4. redevelopment of existing built-up areas, creation of new layouts through mixed land use, adoption of appropriate floor area index (FAI) considering the level of existing and scope for improvement of infrastructure and basic amenities, which helps in keeping the city's growth within

the region's carrying capacity so that urban infrastructure becomes inclusive.

This all entails efficient decision-making through integrated land-use planning as per the city's requirements considering mobility, etc., to minimize mobility related to jobs; enhancement of the functional capacity through user-friendly and economic public transport support; development of mass rapid-transport systems for easy mobility within and between cities; effective use of ICTs as enabling technologies to improve the level of services. This is a welcome measure as most cities are in civic and financial disarray because of unplanned rapid urbanization. Environmentally sound urban centers with essential basic amenities and advanced infrastructures (such as sensors, electronic devices, and networks) would stimulate sustainable economic growth and improvements in services to citizens. The deployment of information and communication technology infrastructures for effective governance support social and urban growth through improved economy and active participation of citizens. Indian cities, while exhibiting technological innovations and connectedness, should also focus on increased living comfort through adequate infrastructure and essential basic amenities to every citizen.

ACKNOWLEDGMENT

SEE ALSO: Cities in Developing Countries; Digital Cities; Global City; Global South/North; Globalization; Spatial Analysis; Sprawl

REFERENCES

Aithal, B. H., and T. V. Ramachandra. 2016a. "Modelling Urban Dynamics of Bhopal, India." *Journal of Settlements and Spatial Planning*, 7(1): 1–14.

Aithal, B. H., and T. V. Ramachandra. 2016b. "Visualization of Urban Growth Pattern in Chennai Using Geoinformatics and Spatial Metrics." *Journal of the Indian Society of Remote Sensing*, 44(4): 617–633.

Aithal, B. H., S. Vinay, and T. V. Ramachandra. 2014. "Landscape Dynamics Modelling through Integrated Markov, Fuzzy-AHP and Cellular Automata." In *Proceedings of International Geoscience and Remote Sensing Symposium* (IEEE IGARSS 2014), Quebec City Convention Centre, Quebec, Canada, July 13–19, 2014.

Aithal, B. H., B. Vishwanatha, and T. V. Ramachandra. 2015. "Spatial Patterns of Urban Growth with Globalization in India's Silicon Valley." In *Proceedings of National Conference on Open Source GIS: Opportunities and Challenges Department of Civil Engineering*, IIT (BHU), Varanasi, October 9–10, 2015.

Karnataka Human Development Report, 2005. Government of Karnataka. Accessed December 20, 2017, at http://planningcommission.nic.in/plans/stateplan/sdr_pdf/shdr_kar05.pdf.

Ramachandra T. V., B. H. Aithal, and B. Barik. 2014a. "Urbanisation Pattern of Incipient Mega Region in India." *Tema: Journal of Land Use, Mobility and Environment*, 7(1): 83–100.

Ramachandra, T. V., B. H. Aithal, and S. D. Durgappa. 2012. "Insights to Urban Dynamics through Landscape Spatial Pattern Analysis." *Journal of Applied Earth Observation and Geoinformation*, 18: 329–343.

Ramachandra, T. V., B. H. Aithal, and K. Shreejith. 2015. "GHG Footprint of Major Cities in India." *Renewable and Sustainable Energy Reviews*, 44: 473–495.

Ramachandra, T. V., B. H. Aithal, and M. V. Sowmyashree. 2013. "Analysis of Spatial Patterns of Urbanisation Using Geoinformatics and Spatial Metrics." *Theoretical and Empirical Researches in Urban Management*, 8(4): 5–24.

Ramachandra, T. V., B. H. Aithal, and M. V. Sowmyashree. 2014. "Urban Footprint of Mumbai: The Commercial Capital of India." *Journal of Urban and Regional Analysis*, 6(1): 71–94.

Ramachandra, T. V., B. H. Aithal, and M. V. Sowmyashree. 2015. "Monitoring Urbanization and Its Implications in a Mega City from Space: Spatiotemporal Patterns and Its Indicators." *Journal of Environmental Management*, 148: 67–91.

Ramachandra, T. V., S. Bharath, and B. H. Aithal. 2013. "Spatio-Temporal Dynamics along the Terrain Gradient of Diverse Landscape." *Journal of Environmental Engineering and Landscape Management*, 22(1): 50–63.

Ramachandra, T. V., B. Vishnu, B. H. Aithal, S. Bharath, and U. Kumar. 2011. "Exposition of Urban Structure and Dynamics through Gradient Landscape Metrics for Sustainable Management of Greater Bangalore." *FIIB Business Review*, 1(1): 1–17.

State and District Domestic Product of Karnataka. 2016. Accessed December 20, 2017, at http://des.kar.nic.in/docs/sip/SDP%202016%20Report%20(1).pdf.

FURTHER READING

Ramachandra, T. V., and B. H. Aithal. 2016. "Bengaluru's Reality: Towards Unlivable Status with Unplanned Urban Trajectory." *Current Science*, 110(12): 2207–2208.

Ramachandra, T. V., V. Bajpai, G. Kulkarni, B. H. Aithal, and S. S. Han. 2017. "Economic Disparity and CO_2 Emissions: The Domestic Energy Sector in Greater Bangalore, India." *Renewable and Sustainable Energy Reviews*, 67: 1331–1344.

Sudhira, H. S., T. V. Ramachandra, and M. H. Bala Subrahmanya. 2007. "Bangalore." *Cities*, 24(5): 379–390.